

# Performance Prediction of the TMT Secondary Mirror Support System

Myung K. Cho\*

GSMT Program Office, National Optical Astronomy Observatory  
950 N. Cherry Ave., Tucson, AZ, USA 85719

## ABSTRACT

The Ritchey-Chrétien (RC) design of the Thirty Meter Telescope (TMT) optics calls for a 3.1 m diameter Secondary Mirror (M2), which is a large meniscus convex hyperboloid. The M2 converts the beam reflected from the  $f/1$  primary mirror into an  $f/15$  beam for the science instruments. The M2 Mirror (M2M) has a mass of approximately two metric tons and the mirror support system will need to maintain the mirror figure at different gravity orientations. Recent changes in the telescope configuration to RC from Aplanatic Gregorian (AG) prescription and reduction of the fully-illuminated field of view to 15 arc minutes required a design change in the M2 mirror figure from a concave radius to a convex radius, with a significant reduction in diameter, which in turn requires re-optimization of the mirror support systems. The optical performance evaluations were made based on the optimized support systems resulting from the change from AG to RC. The M2 optimized support system consists of 60 axial supports, mounted at the mirror back surface, and 24 lateral supports mounted along the outer edge. The predicted print-through errors of the M2M supports are 10nm RMS surface for axial gravity and 2nm RMS surface for lateral gravity. This M2M support system has an active optics capability to accommodate potential mechanical or thermal errors; its performance to correct low-order aberrations has been analyzed. A structure function of the axial gravity support print-through was calculated.

**Keywords:** Secondary mirror, mirror performance, mirror support optimization, active optic, Structure function

## 1. INTRODUCTION

The optical systems of TMT have stringent requirements to achieve scientific goals. The M2M support system was optimized to meet the requirements defined in “TMT Image Size and Wavefront Error Budgets Volume 1, 2, 3”<sup>[4]</sup>. Preliminary wavefront error budget allocation for the M2M figure, from mirror supports (before active optics and adaptive optics corrections), are as follows: 57nm RMS at Zenith and 73nm RMS at 65 degrees elevation. To fulfill the optical and mechanical performance requirements, extensive finite element analyses using I-DEAS and optical analyses with PCFRINGE have been conducted. Mechanical and optical analyses performed include static gravity induced deformations, natural frequency calculations, and support system sensitivity evaluations. An influence matrix was established to compensate potential errors using an active optics system. Performances of the M2M support system were evaluated for the sample sensitivity cases before and after active optics corrections.

As a baseline RC configuration in this study, the M2M was modeled based on the optical prescription in Table 1. The physical and material properties used in FE mirror models are summarized in Table 2.

Table 1. Optical Prescription of TMT in RC.

<b>Primary Diameter</b>	30.0 m	<b>ROC</b>	<b>K</b>	<b>Distance between optics</b>
<b>Primary F ratio</b>	1.0	<b>Primary</b>	-60.00000 -1.000953	<b>M1 - M2</b> 27.0938 (m)
<b>System F ratio</b>	15.0	<b>Secondary</b>	-6.22768 -1.318228	<b>M2 - M3</b> 23.5938
<b>FOV</b>	15 arcmin	<b>Tertiary</b>	flat	<b>M3 - Image</b> 20.0000
<b>M1 to EL</b>	3.5 m			<b>M3 - M1</b> 3.5000

\* [mcho@noao.edu](mailto:mcho@noao.edu); phone 1 520 318-8544; fax 1 520 318-8424; [www.noao.edu](http://www.noao.edu)

# Performance Prediction of the TMT Secondary Mirror Support System TMT.OPT.JOU.08.001.REL01

Table 2. Material properties used in FE mirror models.

Coefficient of thermal expansion	$15 \times 10^{-9} \text{ m/m}^\circ\text{C}$
Thermal conductivity	$1.3 \text{ W/m}^\circ\text{C}$
Specific heat	$766 \text{ J/kg}^\circ\text{C}$
Density	$2205 \text{ kg/m}^3$
Modulus of elasticity	$9.2 \times 10^{10} \text{ Pa}$
Poisson's ratio	0.17

## 2. SECONDARY MIRROR CONFIGURATION

The M2M is a large meniscus convex hyperboloid. The M2M converts the beam reflected from the  $f/1$  Primary Mirror (M1M) into an  $f/15$  beam for the science instruments. A design concept of the M2 Cell Assembly (M2CA) developed by the National Optical Astronomy Observatory (NOAO) is shown in Figure 1 (a). The M2CA consists of M2M, support system, and the cell. Several different FE models were created to serve various calculations. A typical FE mirror model of M2M is composed with four layers of elements with a total of 10,080 solid elements and 12,245 nodes. This model assumes a solid convex meniscus mirror with a diameter of 3.120m, 100mm thick, and a radius of curvature of -6.4m (best fit sphere). The M2M mass was estimated as 1934Kg from the FE solid model shown in Figure 1(b). A local coordinate system in the FE model was assumed as follows: (1) the positive Z-axis corresponds to the line which connects the vertex of the primary mirror to the vertex of the secondary mirror in the telescope; (2) the positive X-axis corresponds to the telescope's mechanical elevation axis; (3) the positive Y-axis is defined by the right hand rule.

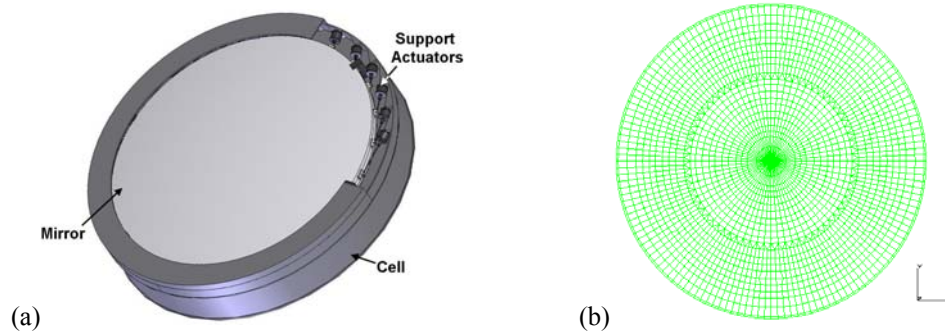


Fig. 1. Secondary mirror Cell Assembly and an M2 finite element model. (a) M2 Cell Assembly (M2CA) consisting of M2M, Support system, and Cell, (b) plane view of mirror FE model.

## 3. M2 SUPPORT SYSTEM

The baseline mirror support system developed by NOAO contains a total of 60 axial supports with an active optics capability and 24 passive lateral supports mounted around the outer edge of the mirror. This M2 support system was optimized for minimum gravity induced errors. The axial support was optimized for the telescope at Zenith pointing, and the lateral was optimized at horizon pointing. The optical performance was evaluated for gravity variations between Zenith and Horizon. The active forces were evaluated based on the influence matrix calculated from 60 axial support points. In addition, random support force errors and sample support failure modes were estimated as a part of the sensitivity and tolerance analyses. To predict the mirror stiffness, fundamental mirror frequencies were calculated with a free-free boundary condition. Active optics correction was attempted to low order Zernike modes to demonstrate the M2M figure corrections. Detailed mechanical and optical performance analyses were conducted using I-DEAS finite element analysis program and the PCFRINGE optical program.

### 3.1 M2M AXIAL SUPPORT

Parametric modeling iterations were conducted for the support system optimization. These iterative calculations utilize an optimization scheme for a minimum global surface deformation over the optical surface. The key metric, during the optimization process, was the optical surface RMS error. This optimization process was initially developed for the Gemini 8m telescopes<sup>[1]</sup> and applied to the Gemini primary mirrors.

In order to achieve the optical performance goal of 20nm RMS surface, extensive parametric calculations were made for an optimum axial support system. The axial support optimization yields an optical surface RMS error of 10nm with a PV of 49nm. This optimized axial support features a 60 axial support system arranged in a four (4) concentric ring pattern. This support optimization involves two main optimization processes to achieve the goal. First, the support locations were determined for a minimum global RMS surface error without constraining support force magnitudes. Next, a further optimization was processed to select support forces into groups without sacrificing the RMS surface errors. Grouping supports will elevate manufacturing and design processes, and results in smaller part counts. The axial support forces were optimized in two groups, nominally 251N on the innermost ring and 323N on the rest. The optical surface contour map and the axial support forces (color coded for force magnitudes) are shown in Figures 2(a) and (b), respectively. The M2M baseline axial support system descriptions and its configuration are summarized in Table 3.

Table 3. The axial support system configuration.

Ring	Radial position (m)	No. of Supports	Support Force (N)
1	0.274	6	250.5
2	0.645	12	323.1
3	1.019	18	323.1
4	1.402	24	323.1

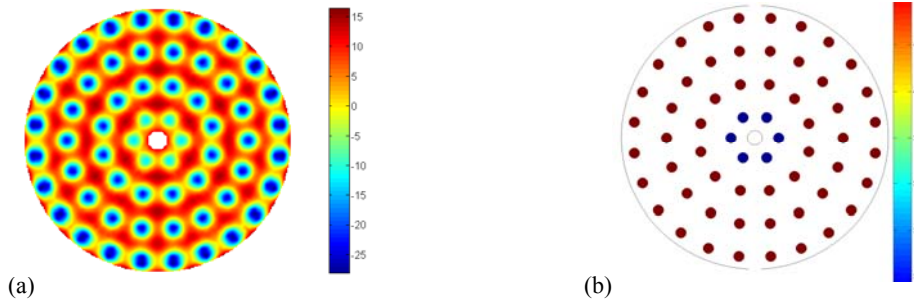


Fig. 2. Axial support print through and optimized support forces. (a) Axial support print through (RMS=10nm, surface), (b) Two axial support forces (250N and 323N).

TMT plans to have the support print through polished out for telescope zenith pointing; therefore, the negative of the axial support print through will appear as the telescope moves away from the zenith in proportion to  $(1-\cos(Z))$ , where  $Z$  is a zenith angle.

### 3.2 M2M Lateral Support

The TMT RC design and M1 segment configuration shows an M2CA shadow of 3.5m in diameter at the M1M central obscuration. This obscuration enables us to develop a lateral support which can be mounted along the outer edge of M2 ( $D=3.1m$ ). This lateral support concept was employed in the Gemini 8m telescopes, VLT 8m telescopes, and currently is being applied to the ATST lateral support design and development.

Performance Prediction of the TMT Secondary Mirror Support System  
TMT.OPT.JOU.08.001.REL01

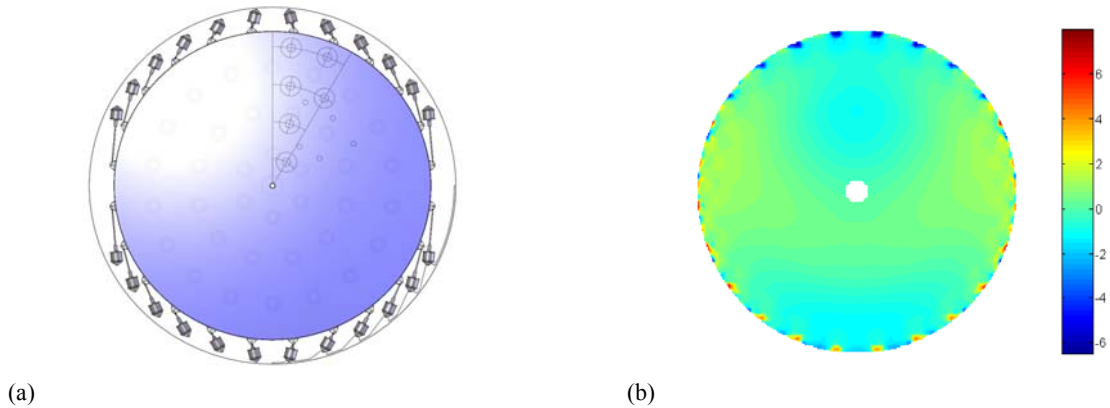


Fig. 3. Lateral support layout and lateral gravity print through error. (a) 24 Lateral support layout (D=3.5m outer diameter shown), (b) Lateral support print through (RMS=2nm surface).

The TMT M2M baseline lateral support configuration developed by NOAO has 24 lateral supports equally spaced along the periphery of the mirror mounted at the M2M mid-plane of the edge. The number of supports and locations were selected based on a trade study by balancing the force directions and magnitudes. Utilized for this trade analysis was a full 3D solid mirror model containing 132 unit influence cases (60 axial supports and 3 degrees of freedom for each of 24 lateral supports). The lateral support optimization was processed based on the following design constraints: (1) no constraints on lateral force magnitudes, (2) self equilibrating support forces to lateral gravity, and (3) minimum application of active forces<sup>[1],[2]</sup>. In this study, additional weights of mount pad and linkage were not included in lateral support optimizations.

The optical surface error due to gravity, at horizon pointing position, was optimized for a minimum RMS surface error. The optimized lateral support was obtained with the optical surface error of 2nm, RMS and 14nm, P-V. This configuration does not require axial forces. The optical surface RMS error can be further reduced to 1.5nm if corrected with active optics forces of 1N or less. The optical surface map and axial forces from the lateral support optimization are shown in Figure 3.

If M2M was polished, figured, and tested at its face down position at Zenith, then no gravity support error would exist at Zenith. At a 65 degrees Zenith position, the support gravity print-through would be a surface RMR of 6nm. The support system adequately meets the optical performance requirements (57nm RMS at Zenith and 73nm RMS at 65 degrees elevation).

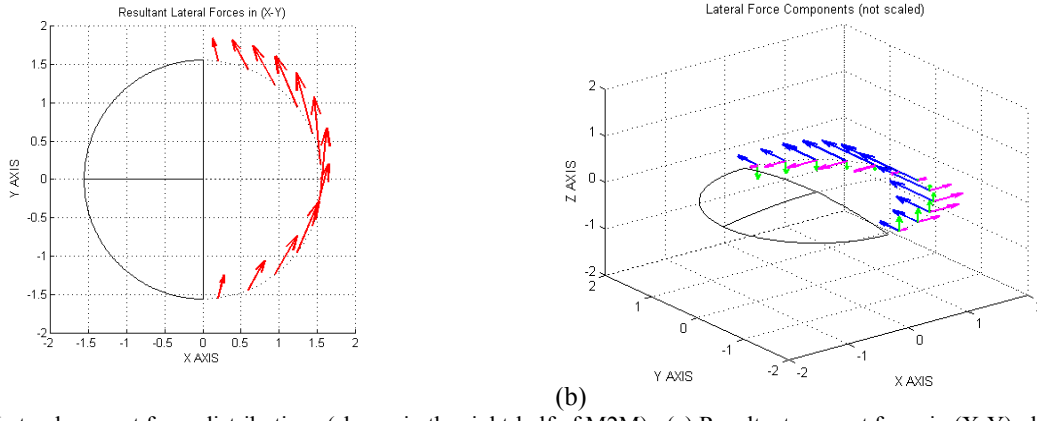
Table 4. Optimized support force components and direction cosines (listed for 12 locations in the right-half of M2M).

Support ID	ANGLE (degree)	Fx (N)	Fy (N)	Fz (N)	(X-Y)x (degree)	(X-Y)y (degree)	(Y-Z)y (degree)	(Y-Z)z (degree)
1	-82.5	97.88	400.76	97.15	76.28	13.72	13.63	76.37
2	-67.5	284.93	510.10	91.49	60.81	29.19	10.17	79.83
3	-52.5	388.60	682.25	77.03	60.33	29.67	6.44	83.56
4	-37.5	382.62	890.74	60.34	66.75	23.25	3.88	86.12
5	-22.5	280.62	1077.71	38.66	75.41	14.59	2.05	87.95
6	-7.5	108.32	1176.08	11.76	84.74	5.26	0.57	89.43
7	7.5	-108.32	1176.08	-11.76	95.26	5.26	0.57	90.57
8	22.5	-280.62	1077.71	-38.66	104.59	14.59	2.05	92.05
9	37.5	-382.62	890.74	-60.34	113.25	23.25	3.88	93.88
10	52.5	-388.60	682.25	-77.03	119.67	29.67	6.44	96.44
11	67.5	-284.93	510.10	-91.49	119.19	29.19	10.17	100.17
12	82.5	-97.88	400.76	-97.15	103.72	13.72	13.63	103.63

# Performance Prediction of the TMT Secondary Mirror Support System

## TMT.OPT.JOU.08.001.REL01

The optimized support forces are also listed in Table 4. The table shows the force components ( $F_x$ ,  $F_y$ , and  $F_z$  in the M2 local coordinate system) and their direction cosines. Direction cosines of the resultant forces at each lateral support were calculated in the (X-Y) and (Y-Z) planes. For example, (X-Y) $\theta$  stands for the resultant force direction (in degrees) measured from Y axis in the (X-Y) plane. Graphical representations of the lateral forces are shown in Figure 4.



(a) (b)  
Fig. 4. Lateral support force distributions (shown in the right-half of M2M). (a) Resultant support force in (X-Y) plane; (b) Force components ( $F_x$ ,  $F_y$ ,  $F_z$ ; not scaled).

Since each lateral support carries a high resultant force as a point load, a local effect due to this lateral force was examined. This local effect (called Poisson's effect) was calculated by applying the optimized lateral force at each of the 24 lateral support locations. This is an important parameter in defining the clear aperture of the M2M. As a first order approximation, the Poisson's effect was estimated by examining the relative displacements between the top and bottom of the mirror surface under the lateral gravity carried by the lateral supports. A maximum local deformation of 19nm was calculated at the lateral support locations and shown in Figure 5. The Poisson's effect was drastically reduced at radial distances of 30mm away from the edge of the mirror. The corresponding maximum surface displacement is 10nm. The maximum stress level was calculated for Von Mises Stress. A maximum stress of  $1.2 \times 10^6 \text{ N/m}^2$  (170 psi) was found under a steel pad of 50x180x5mm at the lateral support locations near the X-axis. The physical dimension and material choice of the support pad will be revisited by advanced opto-mechanical and thermal analyses.

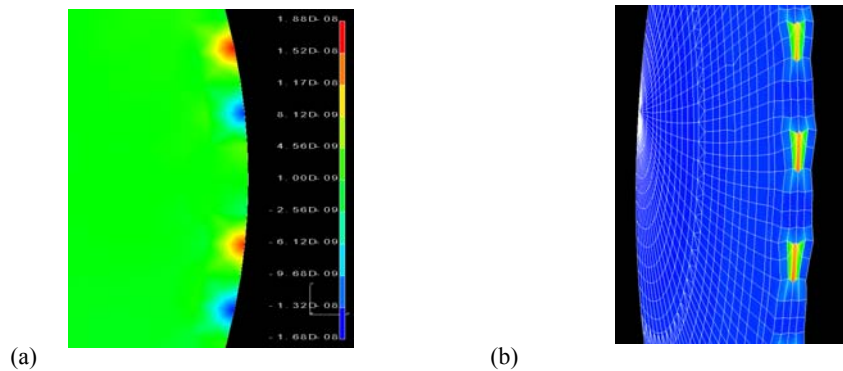


Fig. 5. Poisson's effect at the edge of the M2M due to lateral support force. (a) Localized deformation, (b) Von Mises stress of  $1.2 \times 10^6 \text{ N/m}^2$  (170 psi) at lateral support pads.

### 3.3 Support Sensitivity

Sensitivity and tolerance analyses were performed to quantify the optical surface deformations affected by uncertainties in the design and potential errors involved in polishing, assembly and system integration. The analyses include cases such as: single support failure, single actuator force error, lateral support force errors, and random active force errors. As

Performance Prediction of the TMT Secondary Mirror Support System  
TMT.OPT.JOU.08.001.REL01

a sample axial support failure mode, a single axial support on the fourth ring was assumed to fail, resulting in zero axial force. In this case, the net change of 28nm surface RMS was calculated after re-optimizing the remaining 59 active supports. The optical surface errors are shown in Figure 6.

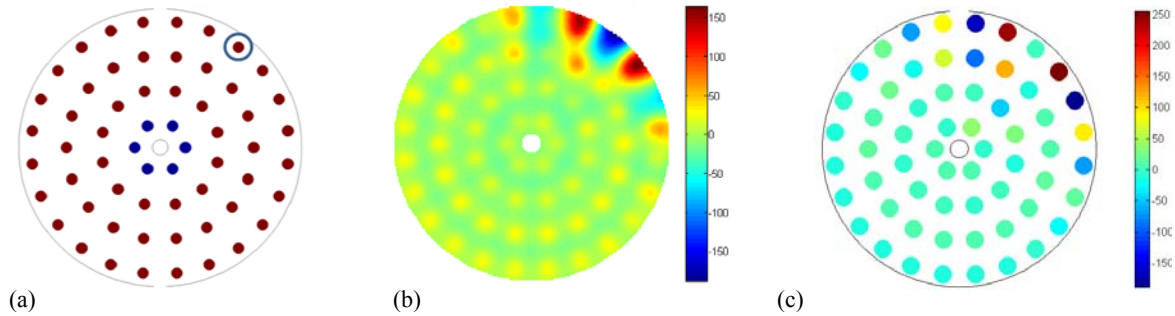


Fig. 6. The optical surface error due to single support failure (active optics system turned on). (a) Supports with a failed actuator marked in a circle, (b) Optical surface error map, RMS = 28 nm, (c) Active force distribution, Fmax= 250N; Fmin= -160N.

For a case in which a single axial support has a force error of 1 N, the net change in the optical surface RMS error is nominally 4nm, after piston, tilts, and focus are removed. This can also simulate one of the axial actuators malfunctioning and having 1N higher than designed force. The optical effect can be scaled linearly since this is a linear FE analysis. The surface error for this unit support force error is shown in Figure 7.

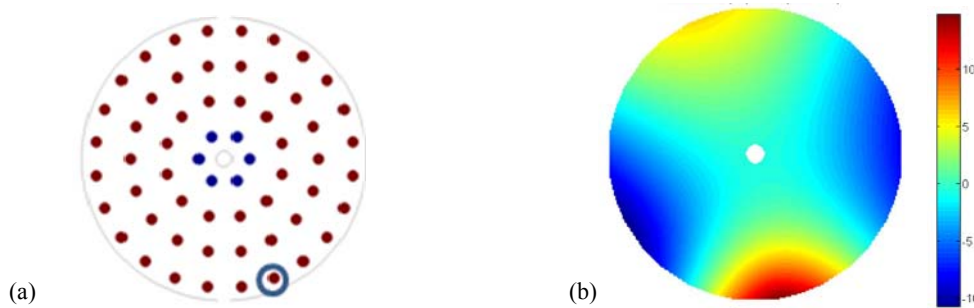


Fig. 7. The optical surface map due to a single support force error of 1N after piston, tilts, and focus are removed. (a) Single support which has a force error of 1N shown in a circle, (b) Optical surface error map, RMS = 4 nm.

The line of action of the lateral support force exerted by each lateral support lies on the mid-plane of the M2M. Any excessive force component of the resultant force will result in upsetting the force balance. For a case in which a single lateral support has a force error of 1 N, in the optical axis (Fz, force in the Z-axis) at a support location (L10), the net change in the optical surface error yields a surface RMS of 7.8 nm. This can be corrected almost entirely by the active optics with a residual optical surface RMS error of 0.1nm. For a case in which a single lateral support has a force error of 1 N, in either X or Y (Fx or Fy), the net change in the optical surface RMS error is less than 1 nm, which can also be corrected, almost entirely, by the active optics. The optical surface distortions from these lateral force errors are shown in Figure 8. For these lateral force sensitivity calculations, considered was the support located at 52.5 degrees, support ID=10 (L10) in Table 4.

Similarly, lateral support position tolerance errors can be estimated by superimposing effects from unit cases of force and moment. For the case in which a single lateral support is misplaced by 1mm along the optical axis, the net change of surface RMS error can be estimated by applying an equivalent load set as a combination of unit force and offset moment at the specific support location.

Performance Prediction of the TMT Secondary Mirror Support System  
TMT.OPT.JOU.08.001.REL01

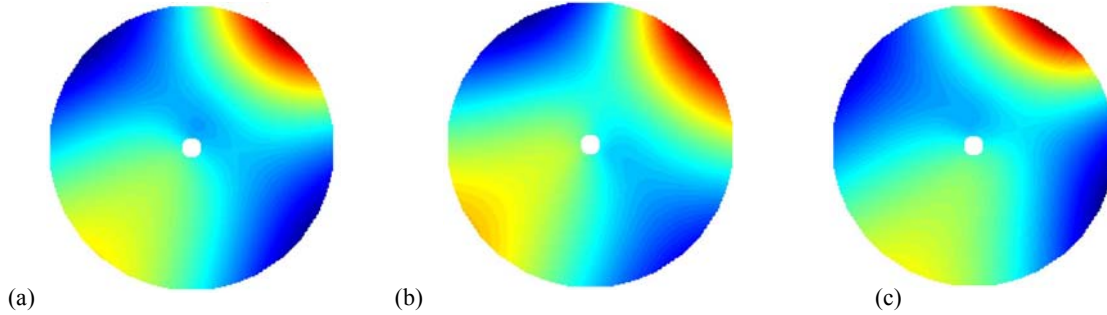


Fig. 8. Optical surface RMS error maps due to lateral support force errors of 1N at a support location (L10).  
(a) 7.8 nm RMS, by Fz, (b) 1.0 nm RMS, by Fx, (c) 1.0 nm RMS, Fy.

Axial support force sensitivity calculations were made assuming the axial forces in a random distribution. This case can simulate actuator manufacturing errors, force repeatability limit, or force accuracy. Ten FE models, with a maximum deviation of 0.5 N ( $\pm 0.25$  N) axial force errors, were created. The analyses assumed that each of the 10 force models were in a random three-sigma Gaussian distribution. A histogram of these 10 force distributions, in coded color, is shown in Figure 9(a). The optical surface error maps produced by each force distribution are shown in Figure 9(b), after removing piston, tilts, and focus. The optical surfaces were summarized and listed in Figure 9(c). Results indicate average overall RMS surface errors of 2.7 nm, with predominantly astigmatic shapes.

Lateral support force sensitivity analyses were also performed. Since the lateral support has three force components at each support location, sensitivity calculations were made to each of these three force components. Again, a histogram of 10 force distributions for the lateral support is shown in Figure 10(a), with a maximum deviation of  $\pm 0.25$  N in a random three-sigma Gaussian distribution. The optical surface error maps produced by Fz (force component in the Z-axis) each force distribution is shown in Figure 10(b), after removing piston, tilts, and focus. For this particular case, the optical surfaces were summarized and listed in Figure 10(c). Results indicate an overall average RMS surface error of 3.4 nm, with predominantly astigmatic shapes. Similarly, the optical surface sensitivity, by random variations in Fx and Fy (force component in the X- and Y-axis) was calculated. Due to the high in-plane stiffness of the mirror, the effect is insignificant (overall average RMS surface error is 0.3nm) for both cases.

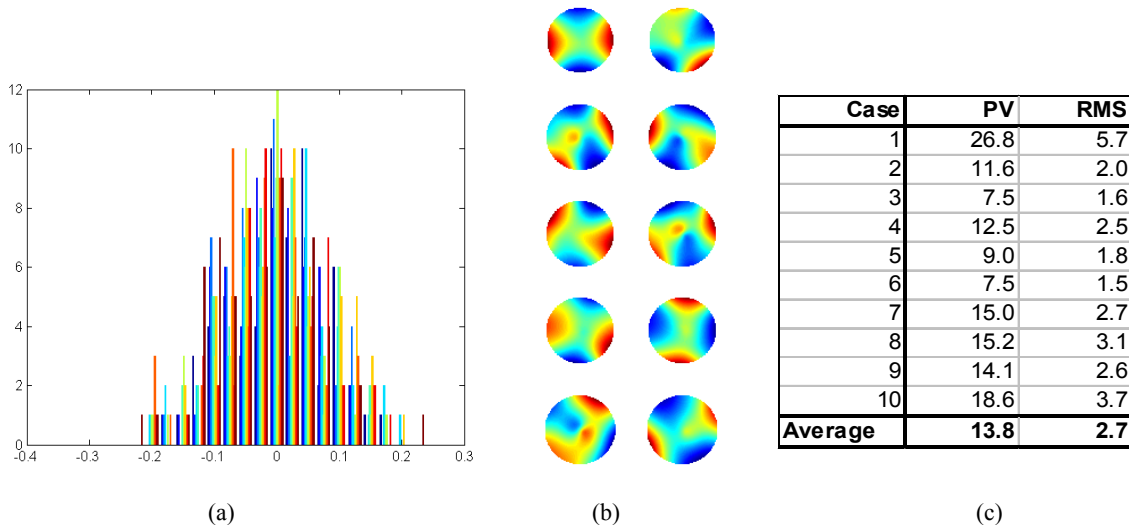


Fig. 9. Axial support force sensitivity (random axial forces in Gaussian distribution). (a) Histogram of random forces (10 modes). Each color represents a force profile distribution. (b) Optical surface responses of 10 random modes. (c) Summary of optical surface RMS errors.

Performance Prediction of the TMT Secondary Mirror Support System  
TMT.OPT.JOU.08.001.REL01

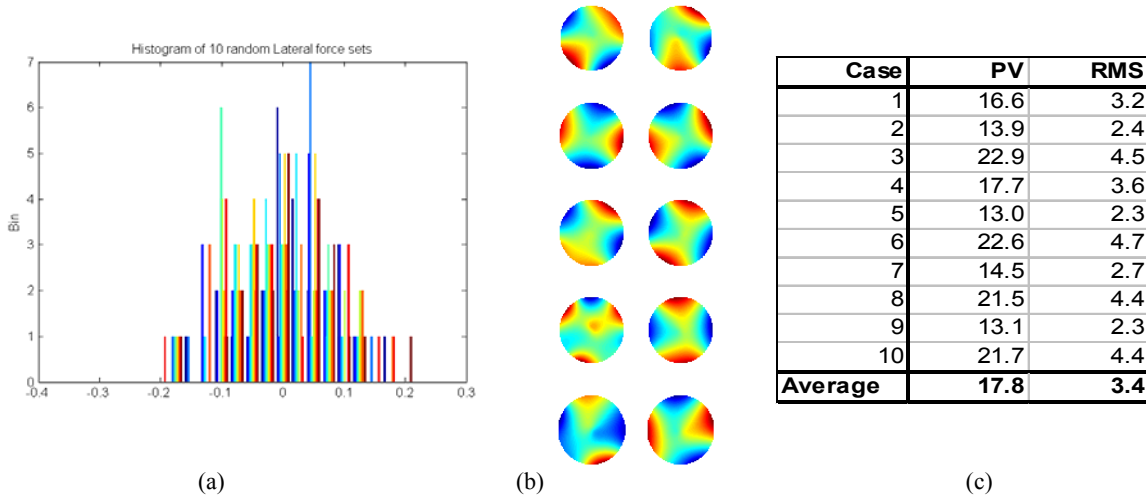


Fig. 10. Lateral support force sensitivity (random Fz forces in Gaussian distribution). (a) Histogram of random forces (10 modes). Each color represents a force profile distribution. (b) Optical surface responses of 10 random modes. (c) Summary of optical surface RMS errors.

#### 4. MIRROR FREQUENCY MODES

Natural frequencies of the mirror were calculated by using a solid full FE mirror model with a free-free boundary condition. These frequency modes are characteristic mirror bending shapes and were obtained after removing rigid body motions (piston and tilts). The natural frequencies, up to 24 modes, were calculated and the first 10 characteristic mode shapes are listed in Table 5. Each of these first 10 characteristic shapes is shown in Figure 11. The lowest mode was found at 64 Hz, as an astigmatic shape. These low frequency modes are similar to low order Zernike polynomials, but not in the same order.

Table 5. The first 10 natural frequency mode shapes.

mode ID	frequency (hz)	mode shape (Zernike equivalent)
1	63.8	0 astigmatism
2	63.8	45 astigmatism
3	145.7	0 trefoil
4	145.7	30 trefoil
5	177.7	focus
6	251.9	0 quadfoil
7	251.9	45 quadfoil
8	271.0	0 coma
9	271.0	90 coma
10	381.0	pentafoil

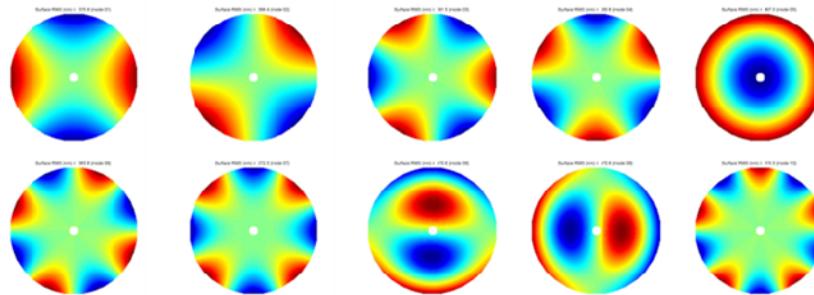


Fig. 11. First 10 natural mirror mode shapes (free-free)

## 5. ACTIVE OPTICS PERFORMANCE

In a seeing limited operation, the M2M optical surface figure errors can be corrected by an active optics (aO) system. The M2M active optics system uses the 60 axial support actuators of the M2M support system. The passive lateral support actuators are not part of the active optics system. A total of 132 unit load (1N) cases (60 axial and 72 lateral cases) are employed to construct an influence matrix for the M2M active optics system.

In order to evaluate the M2M active optics performance, several low order Zernike modes (up to 10 FRINGE Zernike modes)<sup>[8]</sup> were modeled. Each of the first 10 modes (excluding piston, tilts and focus) was scaled to a reference RMS surface error of 1000nm. During the M2 design and development phase at NOAO, the focus was assumed to be adjusted by other compensators. Therefore, the focus correction by M2M aO was disregarded. Figure 12 shows some sample low order Zernike modes. To each individual mode, active optics corrections were applied for a minimum surface RMS error. The performance of aO capabilities for the Zernike modes was summarized in Table 6. In the table, the maximum aO correction forces required to compensate each of 1000 nm RMS surfaces are listed along with the residual surface error and the “aO error” defined as the ratio of the RMS residual error to the RMS input amplitude (1000 nm in each case).

Table 6. Active optics performance with low order Zernike modes in FRINGE order<sup>[8]</sup>

Zernike ID	Raw data		Active Optics Correction			aO error (%)
	P-V (nm)	rms (nm)	P-V (nm)	rms (nm)	Fmax (N)	
4	4715	1000	46.2	6.4	34.8	0.6
5	4825	1000	51.1	6.4	33.0	0.6
6	5506	1000	737.0	87.9	483.3	8.8
7	5506	1000	736.9	87.9	467.1	8.8
8	3337	1000	660.8	171.6	595.9	17.2
9	5535	1000	192.8	22.6	124.8	2.3
10	5535	1000	194.7	22.9	106.4	2.3

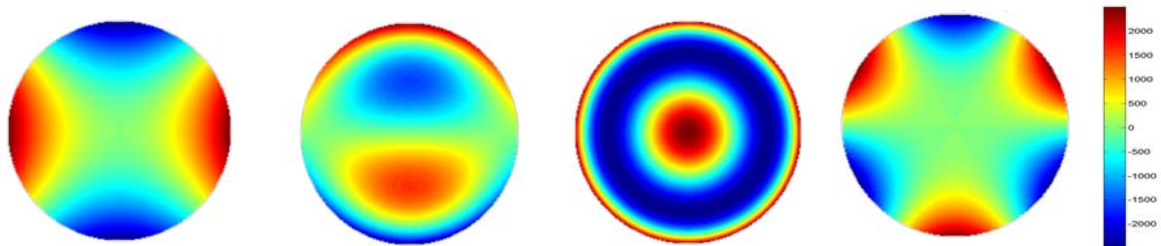


Fig. 12. Sample low order Zernike modes (FRINGE Zernike) used in active optics performances (Z4 and Z5: astigmatism; Z6 and Z7: coma; Z8: spherical; Z9 and Z10: trefoil).

Figure 13 shows an example where the lowest mirror bending mode, an astigmatic optical surface, can be corrected almost entirely. In this case, the astigmatism of 1000nm RMS surface can be reduced to a residual RMS error of 6.4 nm, with a maximum active force of 35 N. It shows an active optics error (aO error) of 0.6%, or 6.4nm/1000nm. This is equivalent to a “gain” of 156, where the “gain” (reciprocal of “aO error”) is defined as the ratio of the surface RMS input amplitude to the surface RMS residual error. The surface map of this lowest mode, residual surface map, and the aO force distribution are shown in Figure 13. The least correctable among these Zernike modes is the spherical mode. The residual RMS surface error of 172nm was calculated and its aO error was 17.2%. This performance analysis indicates that the proposed M2M aO works adequately with the low order aberration modes.

Performance Prediction of the TMT Secondary Mirror Support System  
TMT.OPT.JOU.08.001.REL01

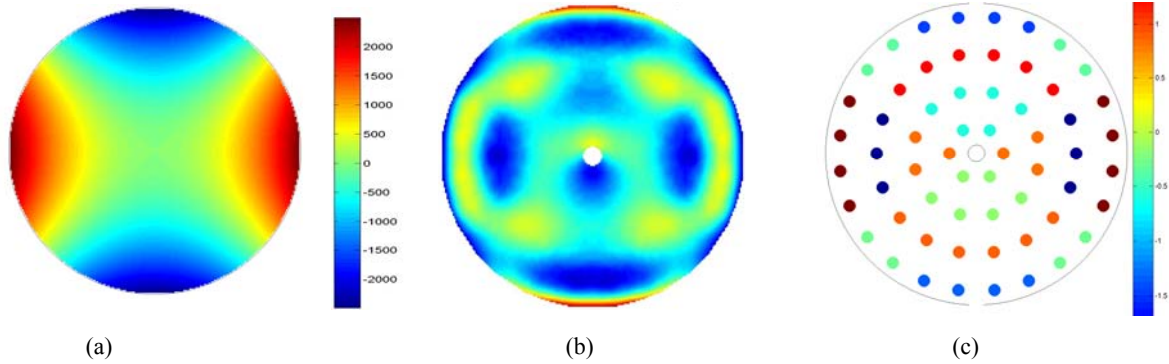


Fig. 13. aO correction to Astigmatism. (a) Astigmatism (Reference): RMS = 1000 nm. (b) Residual RMS surface error (6.4 nm). (c) Active optics force distribution ( $F_{max} = 34.8$  N).

It is desirable to apply the active support system to correct potential errors from external or internal loads after the M2CA is installed in the telescope. For demonstration purposes, two sample cases were modeled to simulate the loading or environmental conditions which can be exerted onto the M2M. These sample cases are: (1) thermal gradients and (2) lateral support force errors.

For the thermal distortions due to temperature variations on the M2M, FE models were created with a unit thermal gradient of  $1^\circ\text{C}$  along each of the local coordinate directions. Modeled, as a most dominant gradient case, was a linear gradient of  $1^\circ\text{C}$  along the thickness ( $1^\circ\text{C}/0.1\text{m}$ ), indicating the top surface  $1^\circ\text{C}$  warmer than the back surface. For this particular case, a P-V surface error of 603 nm and RMS surface error of 175 nm were calculated, after removing piston and tilt. After applying aO correction, the optical surface RMS error was reduced to 4.3 nm with a maximum aO correction force of 15.6 N. The surface error maps before and after aO correction and the correction force distribution are shown in Figure 14. Note that insignificant RMS surface error (less than 1nm) was calculated for thermal gradient cases along the local X or Y-axis after removing piston and tilt before applying aO corrections.

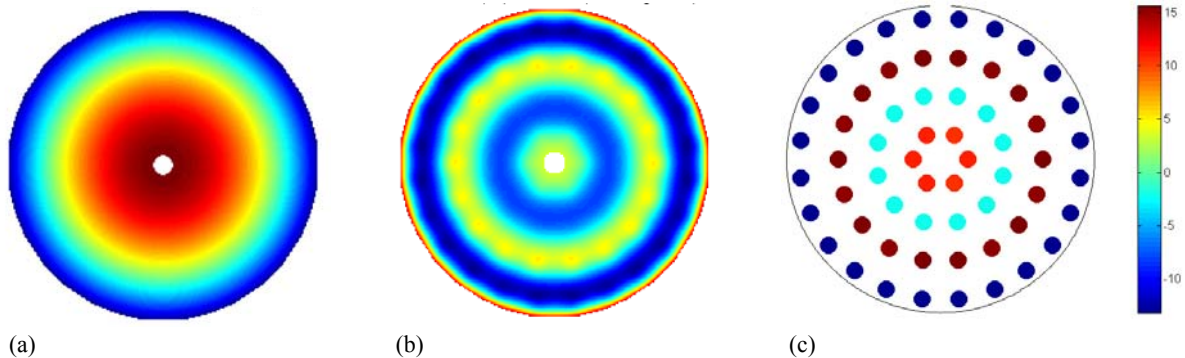


Fig. 14. aO correction to thermal gradient through the thickness. (a) Optical surface map from  $\Delta T$  of  $1^\circ\text{C}$  over a thickness of 0.1m, RMS surface error = 175 nm. (b) Residual RMS surface error = 4.3 nm. (c) aO force distribution ( $F_{max} = 15.6\text{N}$ )

As discussed in the support sensitivity cases, the M2M was deformed into astigmatic shapes when a single lateral support has force errors under lateral gravity load. The effect is especially sensitive when the lateral force has an error along the optical axis (the Z-axis). For the case in which the M2M has a surface RMS error of 7.8 nm, by the lateral force error of 1 N along the Z-axis, the M2M aO can provide efficient correction (residual RMS surface of 0.1nm) with a maximum correction force of 1.2 N. Figure 15 shows the surface maps before and after aO correction and the correction force distribution. Similarly, aO corrections were applied to the lateral support force error cases in the X and Y-axis directions. The errors were almost entirely corrected with low aO forces.

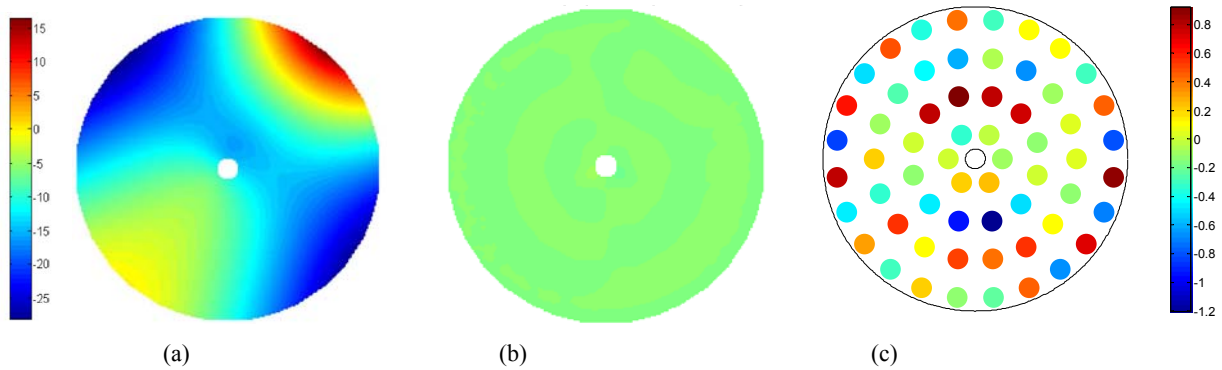


Fig. 15. aO correction for lateral support error of 1 N along the Z-axis under lateral gravity load. (a) Optical surface map from gravity in X, RMS surface error = 7.8 nm, (b) After aO correction, RMS surface error = 0.1 nm, (c) Active optics force distribution (Fmax = 1.2N).

## 6. STRUCTURE FUNCTION

In order to control the amplitude of surface figure errors as a function of their spatial frequency, the M2 System (M2S) Design Requirements Document (DRD) specifies the requirement for surface figure accuracy in terms of a Structure Function (SF). The value of the SF for each separation distance is calculated in terms of the optical path difference (OPD) for each pair of points on the OPD map. SF is defined as:  $D(r) = \langle [\Phi(x+r) - \Phi(x)]^2 \rangle$ , where  $\Phi$  is the OPD at a position  $x$ . A SF was calculated for the axial gravity support print-through at all spatial scales and is shown in Figure 16. For the SF calculation of the M2M, a scale factor of 2 was used to convert the surface error to the OPD. The structure function for gravity print-through was compared to that of the SF requirement in the DRD. The gravity effect is favorably smaller than the requirement by approximately a factor of 10.

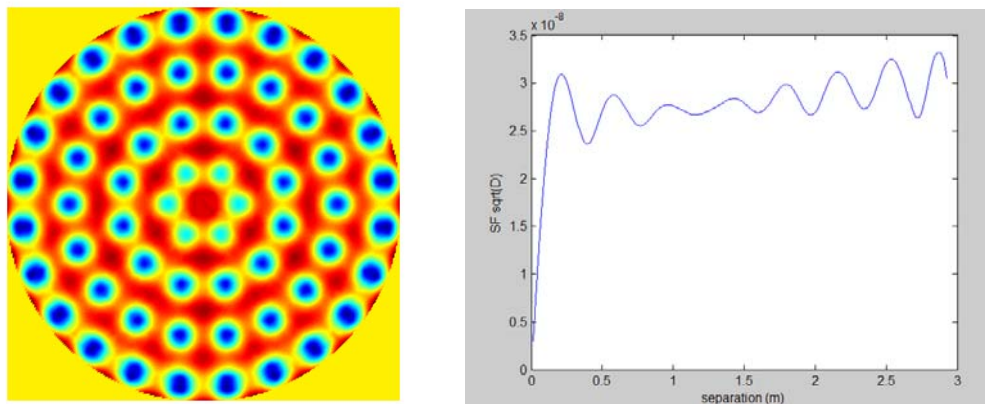


Fig. 16. OPD map of the axial gravity support print-through (10nm RMS surface, or 20nm RMS OPD) and the square root of the structure function,  $D(r)$ , calculated from the OPD map, where:  $D(r) = \langle [\Phi(x+r) - \Phi(x)]^2 \rangle$ .

## 7. SUMMARY

Extensive finite element analyses and optical calculations were performed to optimize a secondary mirror support system for the TMT. In the optimization process, iterative parametric analyses were utilized to achieve a minimum global surface deformation (surface RMS error). The optimized axial support system achieved an optical surface error RMS of

Performance Prediction of the TMT Secondary Mirror Support System  
TMT.OPT.JOU.08.001.REL01

10nm. The axial support system used 60 active axial support actuators, arranged in a four concentric ring pattern. The lateral support system was optimized to achieve an optical surface RMS error of 2nm. The lateral support system used 24 passive lateral supports, equally spaced along the periphery of the mirror mounted at the mid-plane. The optical surface deformations for various Zenith angles were evaluated by combining cases of the effects from axial and lateral gravities. The results showed that the current TMT secondary mirror support system adequately meets the optical performance requirements (57nm RMS at Zenith and 73nm RMS at 65 degrees elevation) and satisfies the M2M surface figure accuracy requirement defined in terms of a Structure Function.

Sensitivity analyses were conducted with several sample cases to quantify the optical surface deformations affected by uncertainties in design and potential errors involved in polishing, assembly and system integrations. A summary of the sensitivity cases described is in Table 7. All of these cases are before aO correction, except the first case, s01. Performances of the M2M aO system were demonstrated using the first 10 Zernike modes. A few sensitivity cases, corrected by the M2M aO, are included in Table 8. The results demonstrated that the M2M aO system is capable of adequately correcting the optical figure errors.

Table 7. Summary of support sensitivity cases.

CASE	PV (nm)	RMS (nm)	REMARK
s01	245.7	28.20	failure axial support at edge (after correction)
s02	28.1	4.40	single axial force error at edge (dF=1N)
s03	5.7	0.97	Force error in single lateral (Fx=1N)
s04	6.2	1.02	Force error in single lateral (Fy=1N)
s05	45.3	7.80	Force error in single lateral (Fz=1N)
s06	13.8	2.70	random axial force error (dF=0.5N)
s07	17.8	3.40	random lateral force error (dF=0.5N)

Table 8. Sensitivity analysis and aO compensation of First 10 Zernike Aberrations.

Zernike ID	Uncorrected		Active Optics Correction			
	P-V (nm)	rms (nm)	P-V (nm)	rms (nm)	Fmax (N)	Gain
4	4715	1000	46.2	6.4	34.8	155.3
5	4825	1000	51.1	6.4	33.0	155.5
6	5506	1000	737.0	87.9	483.3	11.4
7	5506	1000	736.9	87.9	467.1	11.4
8	3337	1000	660.8	171.6	595.9	5.8
9	5535	1000	192.8	22.6	124.8	44.3
10	5535	1000	194.7	22.9	106.4	43.7
Lateral force (Fz)	45.3	7.8	2.1	0.1	1.2	78.0
Thermal gradient	603.0	175.0	19.7	4.3	15.6	40.7

Integrated FE models with the mirror, supports, and mirror cell structure need to be established for further optimizations to refine design parameters of the mirror cell and support systems. A high fidelity finite element model will be required to evaluate more extensive sensitivity cases, structural interaction effects, thermal mismatches, or other opto-mechanical effects. This FE model may include features of support pads, mounting blocks, linkage, and other detail hardware parts which may contribute to mechanical and optical performance degradation.

### ACKNOWLEDGMENTS

This research was carried out at the National Optical Astronomy Observatory, and was sponsored in part by the TMT. The author gratefully acknowledges the support of the TMT partner institutions. They are the Association of Canadian

Performance Prediction of the TMT Secondary Mirror Support System  
TMT.OPT.JOU.08.001.REL01

Universities for Research in Astronomy (ACURA), the California Institute of Technology and the University of California. This work was supported as well by the Gordon and Betty Moore Foundation, the Canada Foundation for Innovation, the Ontario Ministry of Research and Innovation, the National Research Council of Canada, the Natural Sciences and Engineering Research Council of Canada, the British Columbia Knowledge Development Fund, the Association of Universities for Research in Astronomy (AURA) and the U.S. National Science Foundation.

The author would like to acknowledge Laurie Phillips of the GSMT Program Office of NOAO and Ben Platt, Curtis Baffes, Eric Williams, and Larry Stepp of the TMT Project for their review and helpful comments.

## REFERENCES

- [1] Cho, M.K. and Price, R.S., "Optimization of Support Point Locations and Force Levels of the Primary Mirror Support System," RPT-O-G0017, Gemini Technical Report, November, (1993).
- [2] Schwesinger, G., "Lateral Support of very large telescope mirrors by edge forces only," J. of Modern Optics Vol. 38, NO. 8, 1507-1517 (1991).
- [3] Cho, M.K. and Roberts, J.L., "Response of the Primary Mirror to Support System Errors," RPT-O-G0021, Gemini Technical Report, November, (1993).
- [4] Mast, T., "[TMT Image Size and Wavefront Error Budgets Volume 1 2, 3](#)," TMT.OPT.TEC.07.001, (2007).
- [5] Blanco, D., Cho, M., Daggert, L., Daly, P., DeVries, J., Elias, J., Fitz-Patrick, B., Hileman, E., Hunten, M., Liang, M., Nickerson, M., Pearson, E., Rosin, D., Sirota, M. and Stepp, L., "[Control and support of 4-meter class secondary and tertiary mirrors for the Thirty Meter Telescope](#)," *Opt mechanical Technologies for Astronomy*, ed. E. Atad-Ettedgui, J. Antebi and D. Lemke, SPIE Proc. 6273, TMT.OPT.JOU.06.002, (2006).
- [6] Cho, M.K., "[Performance Prediction of TMT Secondary Mirror](#)," Ritchey-Chrétien design, TMT.OPT.TEC.07.027.REL01, (2007).
- [7] TMT, "TMT M2 System Design Requirement Document (DRD)", TMT.OPT.DRD.07.004.CCR28, (2007).
- [8] Cho, M.K. and Richard, R.M., "PCFRINGE Program – Optical Performance Analysis using Structural Deflections and Optical Test Data," Version 3.5, the Optical Sciences Center, University of Arizona (1990).